Master's Thesis – master Energy Science

Assessing the performance of the Utrecht Science Park PV system

Michiel Bruinewoud m.bruinewoud@students.uu.nl
+31657673334

June 4, 2017

Supervisor:
Dr. W.G.J.H.M van Sark

Second reader :
Dr. A Louwen

Abstract

In this research, the performance of and the correlation between the PV systems on Utrecht Science park were analysed. To assess performance, key performance indicators such as specific yield, performance ratio and self-consumption were calculated and compared to similar research and benchmarks. It was found that with a specific yield of 855 kWh/kWp, the systems performs slightly below average for The Netherlands. However, for the Utrecht area, the specific yield is as expected. An average performance ratio of 0.86 ± 0.07 was found, which corresponds well with the benchmark of 0.85 for well-performing systems. Some systems displayed lower performance, part of which can be attributed to inverter clipping and inverter malfunction. The high uncertainty could be greatly reduced by installing pyranometers at every system. 100% self-consumption was found for all except one system, which was expected due to the buildings being office buildings thus having high electricity demand during peak solar hours. One system does not reach 100% self-consumption, however it is not possible to produce a quantitative result for this this system, since no data on electricity delivered back to the grid is available. Strong correlation between the systems was found. All inter-system distances are lower than the decorrelation length of 2.19 ± 0.31 km. When comparing correlation coefficients of the systems with coefficients of inverters of one system, it was found that the total system behaves as one large system. Therefore, in future modelling and forecasting studies, the system can be considered as one large 1.2 MWp system.

Table of contents

1 Introduction

With the global need for renewable energy production and declining prices, photovoltaic (PV) energy production has seen an increase in installed capacity over the last years. In 2017, about 100 GWp of PV capacity was added globally, which is approximately 25% of the 400 GWp total installed capacity at the end of 2017. The majority of the PV systems were installed in China (IEA-PVPS 2018). It is estimated that 815 MWp of PV capacity was added in 2017 in the Netherlands, resulting in a total capacity of 2864 MWp. It is expected that the combined systems will produce 2149 million kWh of electricity, which is about 2% of the total electricity demand in The Netherlands (CBS statline 2018). Figure 1 displays the yearly installed capacity in The Netherlands since 2000.

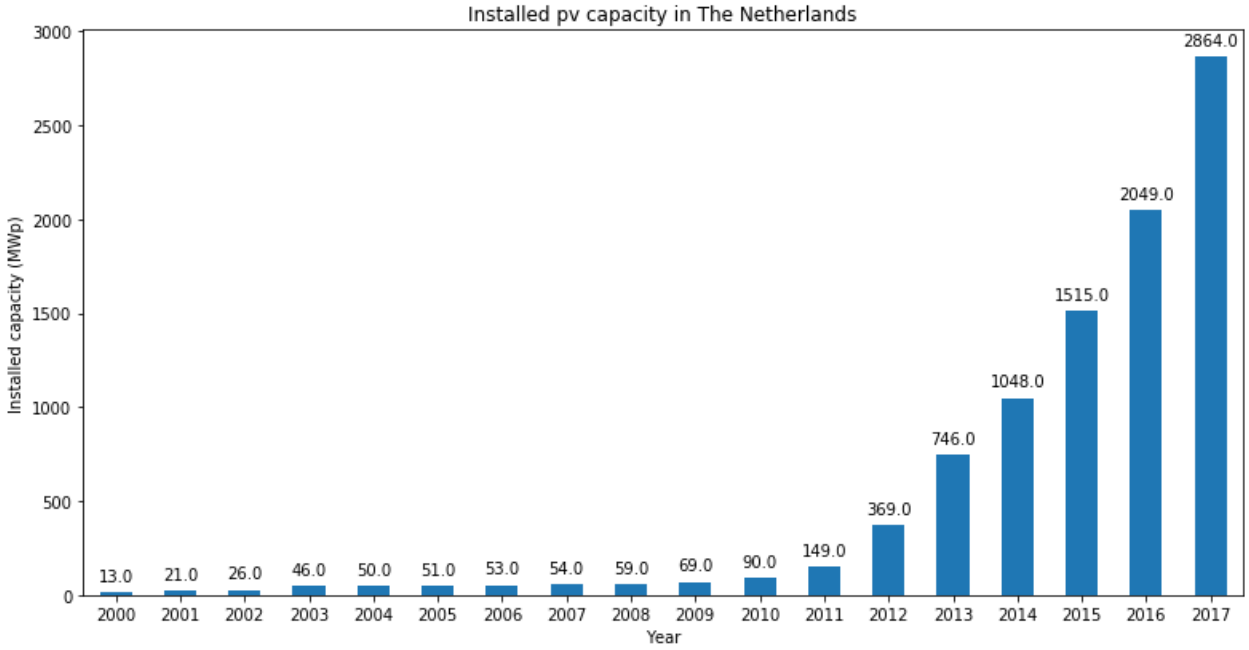

FIGURE 1 INSTALLED PV CAPACITY IN THE NETHERLANDS OVER THE YEARS. THE VALUE FOR 2017 IS AN ESTIMATION. FROM CBS STATLINE

Part of the systems consists of privately owned residential systems, their main purpose being to reduce the electricity bill. To assess whether the systems performs as expected, and thus as a measure to reduce electricity costs, some form of monitoring is required. The most basic form of monitoring consists of measuring the energy production and calculating the annual yield. However, due to varying system size, the expected value for each system is different. A more general performance parameter is the specific yield, which is the annual yield divided by the installed capacity of the system (kWh/kWp). In 2014, the average expected annual yield for the Netherlands was determined to be 875 kWh/kWp (van Sark 2014). However, more recent studies show higher average values of 945 kWh/kWp for 2016 (Moraitis, Kausika et al. 2018). Nonetheless, the value used to calculate by the Dutch statistics bureau Centraal Bureau voor de Statistiek (CBS) is 875 kWh/kWp. Therefore, systems in The Netherlands are considered to perform as expected if their specific yield is equal or higher than 875 kWh/kWp. A more indicative performance indicator is the performance ratio (PR). The PR is an indication of the total system losses due to temperature, efficiency, shading and several other factors. It is the ratio of the actual system yield and the system yield if it were operated under standard test conditions (STC). In general, systems are considered to be performing well when they have a PR of 0.85 (Reich, Mueller et al. 2012). Studies on PR and specific yield of recently installed Dutch and European PV systems show that most systems reach the benchmark values of 875 kWh/kWp and PR=0.85, and thus can be considered well-performing (Kausika, Moraitis et al. 2018; Moraitis, Kausika et al. 2018; IEA-PVPS 2014)

Self-consumption also gives insight in the performance of a PV system. Self-consumption is the fraction of the produced PV energy that is consumed by the building itself. Higher self-consumption is considered better, since there is less need for increased grid capacity and there are less transmission losses. High self-consumption also has a financial advantage. In The Netherlands, a net-metering with feed-in tariff scheme is in place. This means that all self-consumed PV electricity is a saving on the electricity bill. A feed in tariff is paid out on excess PV electricity that is delivered to the grid. This tariff is lower than the electricity price (RVO 2017, IEA-PVPS 2016), thus a higher self-consumption yields a higher return on investment. Typical values for self-consumption of residential PV systems are about 20-30%. For buildings with high electricity consumption during the day, such as industrial or commercial buildings, self-consumption is much higher, possibly as high as 100% (IEA-PVPS 2016).

Power production by PV systems depends on weather conditions such as cloud coverage and is therefore highly intermittent. The increased penetration of PV as a means of power production has increased the intermittency of power production. This increases strain on power networks and on conventional power plants. To keep supply and demand even, the conventional plants must ramp up and down more as the penetration of PV (and wind) increases. To reduce network strain and unexpected ramping, power production of large PV plants and fleets of smaller PV systems like that on Utrecht Science Park can be forecasted (Elsinga, van Sark 2017). Forecasting models for PV fleets rely on knowing the degree of correlation between the power production of each individual system. If the correlation between the systems in the fleet is low enough to smooth out fluctuations, the system may be modelled as one large PV plant (Marcos, Parra et al. 2016). This can make the forecasting of power production less complicated.

1.1 The Utrecht Science Park PV system

Utrecht University (UU) has the ambition to be CO_2-neutral in 2030 (UU ,2017). To reach this goal, Utrecht University has implemented many measures, such as stimulating public transport usage amongst employees and reducing energy consumption. Utrecht University's energy consumption is responsible for half of its carbon footprint. Therefore, supplying this energy demand in a sustainable way has a large potential in reducing the carbon footprint. Part of the UU's energy production is realized by the 4600 photovoltaic (PV) modules that are installed on a small part of UU roofs, comprising a total installed capacity of 1.2 MWp. Each module has a rated capacity of 270 Wp. It is estimated that these panels will produce a total of 1 million kWh of electricity each year, which is about 2% of the yearly electricity demand of UU . The PV-panels are grouped in eight systems, each system installed on a different roof on Utrecht Science Park (USP). The location of each system is displayed in Figure 2.

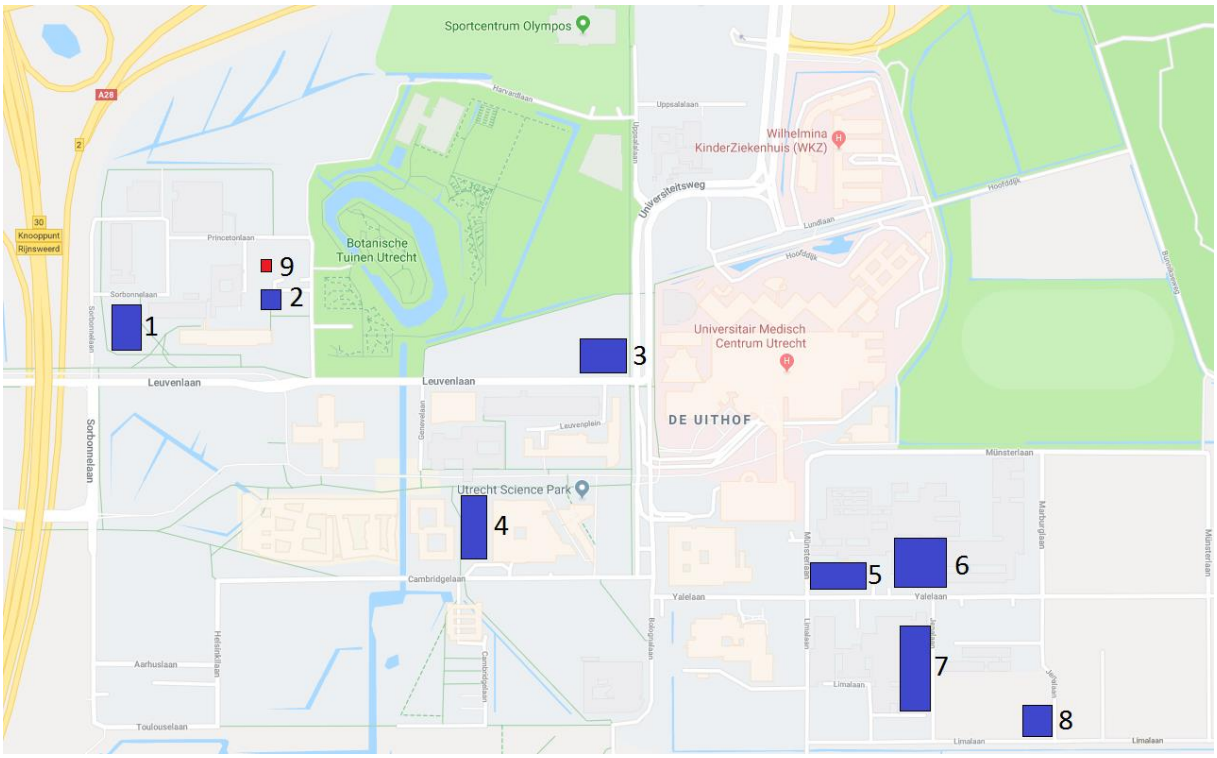

FIGURE 2 THE LOCATION OF EACH PV SYSTEM ON UTRECHT SCIENCE PARK (BLUE). 1: CAROLINE BLEEKER BUILDING (CB), 2: VICTOR J. KONINGSBERGER BUILDING (VJK), 3: DAVID DE WIED BUILDING (DDW), 4: UNIVERSITY LIBRARY (UB), 5: JEANETTE DONKER-VOET BUILDING (JDV), 6: WILLEM C. SCHIMMEL BUILDING (WCS), 7: MARTINUS G. DE BRUIN BUILDING (MDB) ,8: WATERBERGING DIERGENEESKUNDE/TOLAKKER (WGB), 9: UPOT PYRANOMETER

The orientation and tilt of the modules varies among the systems. Module tilt, installed capacity, capacity per orientation are displayed in Table 1.

TABLE 1 IMPORTANT PARAMETERS OF THE SYSTEMS. ALL SYSTEMS ARE INSTALLED ON FLAT ROOFS EXCEPT FOR THE WGB SYSTEM.

System	Installed capacity (kWp)	Orientation (capacity per orientation(kWp))	Tilt (degrees)
CB	132.30	W (72.36), E (59.94)	10
VJK	33.39	S (33.39)	10
UB	232.20	N (116.1), S (116.1)	10
DDW	121.12	W (49.68), S (23.76), E (49.68)	10
JDV	46.44	W (23.22), E (23.22)	10
WCS	233.28	W (116.64), E (116.64)	10
MDB	285.66	W (142.83), E (142.83)	10
WGB	131.22	S (131.20)	30

2 Research aim

The main aim of this research is to assess the performance of each system and the total system. If the performance is lower than expected, a possible explanation for the low performance will be given. The main research questions are:

Do the PV systems at the UU campus perform as expected?
If no: for what reason is system performance below expectations?

To answer these questions, numerous performance indicators will be calculated and compared to results from literature. First of all the annual yield will be compared to the expected yield (1000 MWh) and specific yields will be compared to nation-wide and regional averages. Performance ratios of each system will be calculated and compared with the benchmark value of 0.85 and with results from similar research. Specific yield and PR results will also be compared to earlier research done on this system (van Sark, de Waal et al. 2017). Finally, the self-consumption of PV energy will be calculated. For buildings with high self-consumption the daily ratio of PV/demand will be calculated.
The production and performance data can be used to determine if the production variations of the individual systems correlate. This is the aim of the second part of this research. If the variations do not correlate, the systems may be modelled as a very large PV plant where the variations are smoothed, provided it meets certain conditions. This can reduce the need for individual irradiation measurements for each system, because this model only needs irradiation data from one point(Marcos, Parra et al. 2016). If the systems correlate strongly, the total system may be treated as one single system. The research questions for the second part of this research are:

What is the decorrelation length of the PV system?
How strong is the correlation of system pairs within the decorrelation length?

To answer this, methods from (Elsinga, Van Sark 2013)) will be used to calculate the decorrelation length of the system. For system pairs within the decorrelation length, the degree of correlation will be calculated using the Pearson correlation coefficient.
The methods used to answer the research questions are described in detail the next section.

3 Methods

This section describes the methods used to acquire data and to assess system performance and calculate correlations.

3.1 Data acquisition

Each system is equipped with inverters that transform the dc current to ac current that can be used in the grid and the building itself. Each inverter logs data such as power production and inverter temperature every 5 minutes and transmits this data to a central smart logger through a wireless connection. This data is accessible through the NetEco portal, which provides a clear overview of energy yields and power production. To save storage space, the 5-minute data is averaged over 15-minutes and replaced by this 15-minute data after one month. The data was recorded since the systems were installed in 2016. Another measurement takes place further down the building. Here, the energy produced by the whole system is measured each 15 minutes, as well as the electricity demand of the building. Irradiance data is acquired from the Utrecht Photovoltaic Outdoor Test Facility (UPOT) pyranometer.

3.2 Annual yield and specific yield

The annual yield is calculated by adding the daily yields over the year 2017. The specific yield is then calculated by dividing this value by the system capacity. This is done for the individual system and total system.

3.3 Performance ratio

The key indicator needed to answer the first research question is the performance ratio. The performance ratio (PR) is defined as (Reinders, Verlinden et al. 2017):

$$PR = \frac{Y_f}{Y_r} \tag{1}$$

Where Y_f is the final system yield and Y_r is a reference yield. This reference yield is the amount of power a PV system would produce if it were to always operate under standard test conditions (STC). STC are constant irradiance of 1 kW/m^2 (air mass 1.5 spectrum) and a constant cell temperature of 25 degrees C. Y_f and Y_r are calculated as follows:

$$Y_f = \frac{E_{AC}}{P_{STC}}, Y_r = \frac{H_{POA}}{G_{STC}} \tag{2}$$

With E_{AC} the energy delivered by the system, P_{STC} the total rated capacity of each system (Table 1), H_{POA} the total irradiance in plane of the modules and G_{STC} the STC irradiance of 1kW/m^2. The performance ratio can be calculated for any time period. To assess overall performance, a yearly performance ratio would suffice. PV systems in the Netherlands are generally regarded as performing well when the performance ratio is equal or higher than 0.85 (Reich, Mueller et al. 2012) . The monthly performance ratio can be used to see seasonal variations. This research will be using the daily, monthly and yearly performance ratio as the main indicators for performance. Data for each parameter is available. However, the irradiance and energy measurements have different time resolutions, so some smoothing and resampling of the data points is needed. Furthermore, data for some periods is missing due to malfunctioning data transmission. How the data and their respective uncertainties are obtained is described below.

3.3.1 E_{AC}

As described in section 1, the power production data is sent from the smart logger to the NetEco server through a wireless internet connection. However, this connection malfunctioned numerous times, resulting in gaps and thus incomplete data. For fair comparison of the performance ratio of the systems, only days without any gaps in each system can be used. Each system has had difficulties with data transmission at some point since installation. This resulted in only one third of the data being viable to use for analysis. Using such a small fraction of the total data to assess the total system performance could result in unreliable conclusions. Fortunately, other production meters are installed as well. These are used to measure the energy production of each system. Data from these meters was obtained from the UU energy coordinator. These measurements have a lower time resolution of 15-minutes when compared to the inverter production meters. However, the absence of the aforementioned gaps in this dataset makes it more suitable for performance ratio calculations. Therefore it was decided to use the production meter data instead of the inverter data.
The values given by the production meter are rounded to 1 kWh, meaning that it has an uncertainty of ± 0.5 kWh. However, this is an underestimation of the uncertainty. Having two points where the production is measured (the inverters and production meter) gives an opportunity to compare the two and to base uncertainty on this. By analysing the differences between the daily totals (on days without gaps only) of the inverter data and the daily totals of the production meter, it was found that on average the datasets differ by 2.6% of the production meter data. Possible reasons for this could be conversion losses in the inverters or precision of the inverter measurements. The uncertainty in E_{AC} was taken to be ±2.6%.

3.3.2 H_{POA}

To get accurate data for H_{POA} for each system, pyranometers should be installed in plane with the modules. However, this is not the case for the systems at the UU campus. There is one pyranometer at UPOT, which is close to all the PV systems analysed in this research. This pyranometer measures global (horizontal) irradiance, irradiance at 37 degrees tilt and both direct and diffuse irradiance at a time resolution of 30 seconds. Tools from the PVlib (Holmgren, Andrews et al.) python package can be used to calculate the H_{POA} of each system and orientation using the global horizontal, direct and diffuse data from UPOT and the location, tilt and orientation of each system. As displayed in Table 1 most systems are composed of arrays with different orientations and thus multiple planes of irradiance. The H_{POA} will be calculated for all orientations present in a system. To calculate the performance ratio, a single value for HPOA is needed. This single value is proportional to the amount of modules of each orientation. For example. If a system were to have half of its capacity orientated south and half north, the H_{POA} would be the average of H_{POA} north and H_{POA} south. In general, the in plane irradiance of each system can be written as:

$$H_{POA} = \sum_{i} H_{POA,i} * \frac{cap_i}{P_{STC}} \tag{3}$$

With i the orientations of the system (see Table 1), $H_{POA,i}$ the plane of array irradiance of each respective orientation, cap_i the capacity in that orientation, and P_{STC} the total capacity of the sub system. The UPOT data has some missing data points as well. Using the whole dataset without selecting would result in inaccurate results due to the missing data. Therefore, only the days from the data set that have a data point at least every 15 minutes (the same time resolution as the EAC data) were used in this analysis.
The pyranometer at UPOT has an uncertainty of 2.5% in the irradiance measurements. However, using this in the H_{POA} calculations would result in a underestimation of the uncertainty. This is due to the distance between UPOT and the systems. Some system, such as CB, are relatively close to UPOT while others like WGB are located more than 1.5km from UPOT. Some measure of the difference in irradiance over comparable distance was needed. For this, data from the KNMI was used. The KNMI is located approximately 2 km from UPOT, and it has global horizontal irradiance data available for this location. Therefore, this data can be used as a measure for the difference over distance of ~2 km. It was found that the average difference in total global horizontal irradiation between UPOT and the KNMI was 3.9%. No data for direct and diffuse irradiance is available from the KNMI. Therefore it was assumed that the 3.9% also holds for direct and diffuse irradiance. The total uncertainty for the irradiance data used to calculate H_{POA} is the sum of the uncertainty of the pyranometer and the distance related uncertainty. Thus, the total uncertainty of the irradiance is 6.4%.

E_{AC} and H_{POA} were used to calculate the daily PR of each system. These results were averaged to obtain the average PR of each system. When the yearly performance ratio is significantly lower than expected, there may be flaws in the system. Low performance can have numerous reasons such as poor maintenance or high module degradation, unwanted shading or poor system design. If possible, causes for low system performance will be determined for poor-performing systems. The average PR of the systems was already calculated in (Van Sark, De Waal et al. 2017), but this was done using the data from the inverters which includes the aforementioned gaps. Therefore it was expected that the results from this research deviate significantly from the previously conducted research.

3.4 Self-consumption

The data obtained from the energy coordinator includes the electricity demand of each building, in the same 15-minute time resolution as the PV production data. This data was used to calculate the self-consumption using the following method. First, to calculate the energy *not* consumed by the building, the difference between the PV production and the electricity demand was calculated. When this value was negative, it was set to 0:

$$\Delta E_{t,min} = \begin{cases} E_{AC,t} - D_{E,t} \; if \; E_{AC} > D_E \\ 0 \qquad\qquad if \; E_{AC} < D_E \end{cases} \tag{4}$$

With E_{AC} the PV energy produced at time t and $D_{E,t}$ the electricity demand of the building at time t. The *maximum* self-consumption is then defined as:

$$SC_{max} = \left(1 - \frac{\sum_t \Delta E_{t,min}}{\sum_t E_{AC,t}}\right) \times 100\% \tag{5}$$

This can be calculated for any desired time step, such as a day or a year. In this research, the daily self-consumption was calculated and averaged over the complete time period of the data.
The demand and production data are rounded to 1 kWh. This means that a value of 1.49 and 0.50 are both rounded to 1, while the difference between the values is very close to 1. This rounding introduces uncertainty in the calculation of self-consumption. To calculate the *maximum* amount of energy *not* consumed by the building the same method as above was used with one addition. When $E_{AC,t}$ and $D_{E,t}$ are equal, the difference was set to 1:

$$\Delta E_{t,max} = \begin{cases} E_{AC,t} - D_{E,t} \; if \; E_{AC} > D_E \\ 1 \qquad\qquad if \; E_{AC} = D_E \\ 0 \qquad\qquad if \; E_{AC} < D_E \end{cases} \tag{6}$$

The *minimum* self-consumption is then defined as:

$$SC_{min} = \left(1 - \frac{\sum_t \Delta E_{t,max}}{\sum_t E_{AC,t}}\right) \times 100\% \tag{7}$$

The final self-consumption is somewhere between the values of SC_{max} and SC_{min}. To rewrite the self-consumption as standard $x \pm \sigma$, the self-consumption is defined as:

$$SC = \frac{SC_{max} + SC_{min}}{2} \pm \frac{SC_{max} - SC_{min}}{2} \tag{8}$$

It was expected that the self-consumption of the systems are high. This is due to the building being university (office) buildings, thus having high electricity demand during solar peak hours. However, it is expected that self-consumption drops during summer, when the demand expected to be lower due to summer break. Furthermore, more PV energy is produced, also after working hours. For buildings with high (100%) self-consumption, the daily ratio of PV/demand is calculated using the 15-minute data.

3.5 Correlation

In this research, the degree of correlation for each pair of systems will be determined. Literature proposes various methods for calculating this correlation. Some propose calculating the 'regular' Pearson correlation for the system pairs (Perez, Kivalov et al. 2012)(Perpiñán, Marcos et al. 2013). Others propose the use of dispersion factors (Hoff, Perez 2010). This method requires data on cloud speed and direction, which is not available in this form. Using cloud pictures from UPOT or using wind speed as a proxy for cloud movement entails making many assumptions. This method may result in inaccurate results for the correlation, and is therefore not used. The method used in (Elsinga, Van Sark 2013)) was be used in this research. This method was used in researches on systems similar to that on Utrecht Science Park (randomly spaced urban rooftop PV systems), and is therefore the method most appropriate for this research. This method is discussed in more detail in the next section.

3.5.1 Decorrelation length

As described in the introduction, the inverters log power production P_t each 5 minutes. After a month, this 5-minute data is replaced by 15-minute data. It is assumed that the power production is constant over each time step. Knowing P_t, the variation in power production also known as the ramp rate (RR), at time *t* is:

$$RR_t = P_{t+1} - P_t \tag{9}$$

RR_t can be used to calculate the correlation between the ramp rates of different sub systems. However, most systems have a different system capacity (Wp). For fair comparison, the ramp rates should be normalized. For system *i* the normalized ramp rate is:

$$\overline{RR_{i,t}} = \frac{P_{i,t+1} - P_{i,t}}{W_{p,i}} \tag{10}$$

The correlation is determined for each possible pair i, j in the data set. Pairs with high correlation will have many points where $\overline{RR_{i,t}} = \overline{RR_{j,t}}$,meaning that the variations are equal and at the same time. When plotting $\overline{RR_{j,t}}$ against $\overline{RR_{i,t}}$, these points lay on the line $\overline{RR_{i,t}} = \overline{RR_{j,t}}$. Divergence from this line indicate points where the variations occur on a different point in time or have a different magnitude. The higher the variance perpendicular to this line, the lower the correlation of the system I and j. This variance is displayed in Figure 3

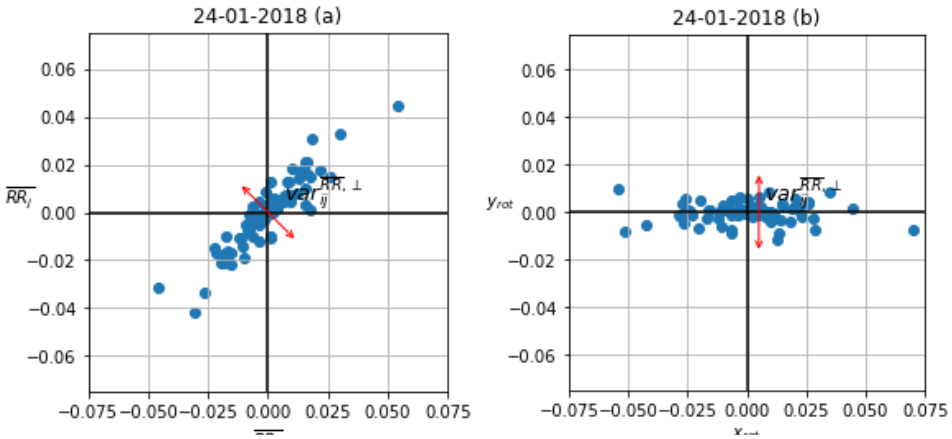

FIGURE 3 SCATTER PLOT OF THE NORMALISED RAMP RATE OF TWO SYSTEMS (A) AND THE ROTATED DATA (B). THE RED ARROW INDICATED THE PERPENDICULAR VARIANCE

To obtain $var_{ij}^{\perp}$, the normalised ramp rate data displayed in Figure 3 (a) was rotated 45° clockwise, resulting in the data displayed in Figure 3(b). This was done by replacing the $\overline{RR_{i,t}}$ (x) and $\overline{RR_{j,t}}$ (y) coordinates with the following parametrisations:

$$x = \frac{x+y}{\sqrt{2}}, y = \frac{x-y}{\sqrt{2}} \tag{11}$$

Since standard deviation is the square root of variance, we now have an expression for the standard deviation:

$$\sigma_{ij}^{\perp} = \sqrt{var_{ij}^{\perp}} \tag{12}$$

Where $\sigma_{ij}^{\perp}$ is inversely related to inter-system correlation. Each pair of systems *i, j* has a specific distance between the systems, D_{ij}. It was assumed that correlation decreases with increasing distance. Exponential decay of correlation with increasing distance was assumed. This exponential decay agrees with the needed auto correlation of a system, when D_{ij} =0. Furthermore, it displays the absence of correlation over large distances. This is required since clouds responsible for the perpendicular variance always have a finite size. This distance-dependency of inter-system correlation was used to define a decorrelation length, which is the distance between the systems over which the correlation has dropped by 95%. This decorrelation length *3b* and the exponential decay are displayed Figure 4. $\sigma_{ij}^{\perp}$ data was fitted to the exponential function to determine the decorrelation length for each day. A plot of this data fitted to the exponential decay function is displayed in Figure 5.

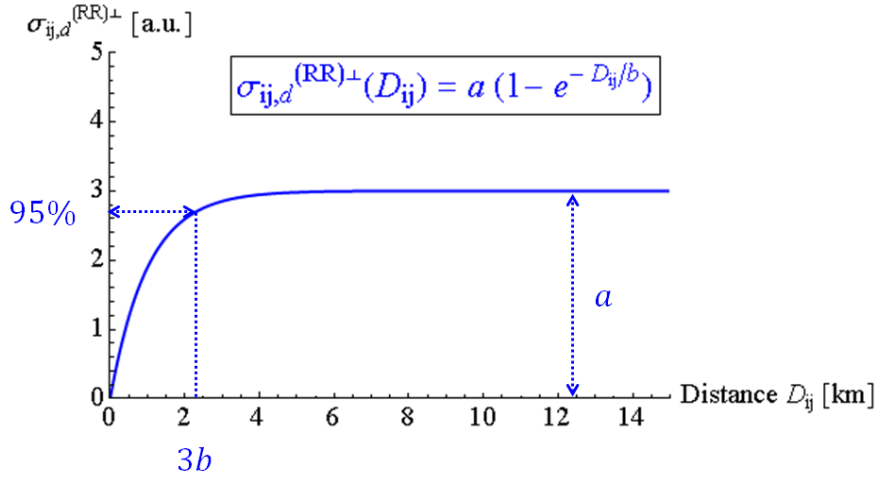

FIGURE 4 EXPONENTIAL DECAY OF THE INTER-SYSTEM STANDARD DEVIATION. 3B, THE DECORRELATION LENGTH, IS THE POINT WHERE THE CORRELATION HAS DROPPED BY 95%. FROM (ELSINGA, VAN SARK, 2013)

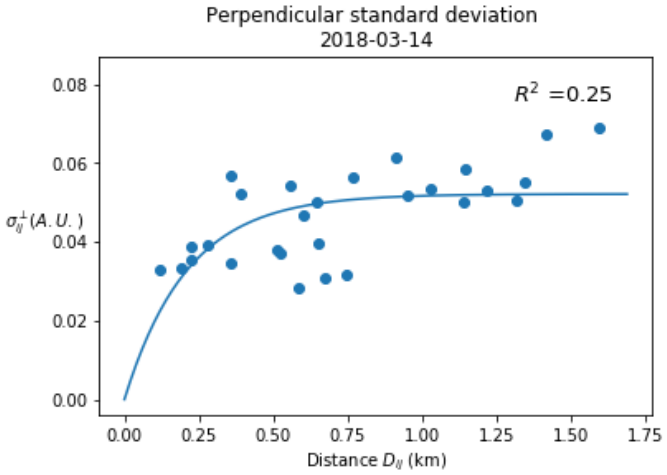

FIGURE 5 Σ_{ij} DATA FITTED TO THE EXPONENTIAL FUNCTION DISPLAYED IN FIGURE 3

For each day in the timespan of the data set, a fit was made. To obtain one value for the decorrelation length the results were averaged. However, to omit bad fits with very low R^2 and thus very high uncertainties, the values of R^2 were used as weighting factors to calculate the weighted average decorrelation length.
For pairs with $D_{ij}<3b$, high correlation was expected. Decorrelation lengths in the order of 1km have been reported for comparable systems and timesteps (Elsinga, Van Sark 2013),(Elsinga, Sark 2015),(Perez, Kivalov et al. 2011). It was expected that many of the systems in this research will have high correlation since the decorrelation lengths found are higher than most inter-system distances at Utrecht Science Park.

3.5.2 Pearson correlation

The degree of correlation was determined for each system with D<3b by calculating the Pearson correlation coefficient of these pairs. In this case, the correlation is defined as:

$$\rho_{ij} = \frac{Cov\left(\overline{RR_{\iota,t}}, \overline{RR_{J,t}}\right)}{\sqrt{Var\overline{RR_{\iota,t}})Var(\overline{RR_{J,t}}\right)}} = \frac{\sum_{t=1}^{T}\left(\left(\overline{RR_{\iota,t}} - \overline{\overline{RR_{\iota}}}\right)\left(\overline{RR_{J,t}} - \overline{\overline{RR_{J}}}\right)\right)}{\sqrt{\sum_{t=1}^{T}\left(\overline{RR_{\iota,t}} - \overline{\overline{RR_{\iota}}}\right)^2 \sum_{t=1}^{T}\left(\overline{RR_{J,t}} - \overline{\overline{RR_{J}}}\right)^2}} \quad (13)$$

Where the double bar on $\overline{\overline{RR_{i,t}}}$ indicates the mean of the normalized ramp rate over t. To omit trend effects due to seasonal variation, the correlation was calculated for each day in the dataset and averaged. Again, this was done for both the 5- and 15-minute data. The results are discussed in the next section.

4 Results

In this section, the results are discussed. The order of subjects from section 3 is maintained.

4.1 Annual yield and specific yield

The yield was calculated using the 15-minute data from the yield meters of each system. The yield since September 2016 is displayed in the figure.

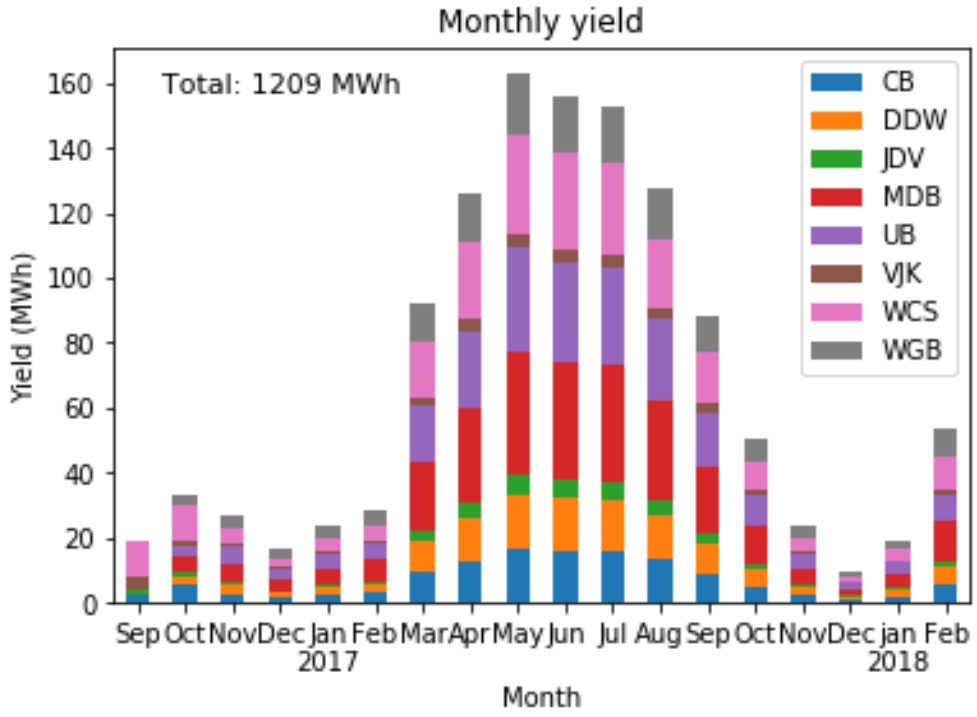

FIGURE 6 SYSTEM YIELD SINCE THE SYSTEMS WERE INSTALLED IN SEPTEMBER 2016. FOR SOME SYSTEMS, ENERGY PRODUCTION MEASUREMENTS STARTED IN NOVEMBER, HENCE THE MISSING OR SMALLER COLOURS IN THE PERIOD SEPTEMBER – NOVEMBER 2016

As can be seen in the figure, the systems with the largest installed capacity (MDB, UB and WCS) have the largest yield. A total of 1209 MWh of energy have been produced between September 2016 and February 2018. 1040 MWh was produced in 2017, which agrees well with the estimated 1000 MWh yearly yield which was expected. The monthly specific yields since September 2016 are displayed in Figure 7.

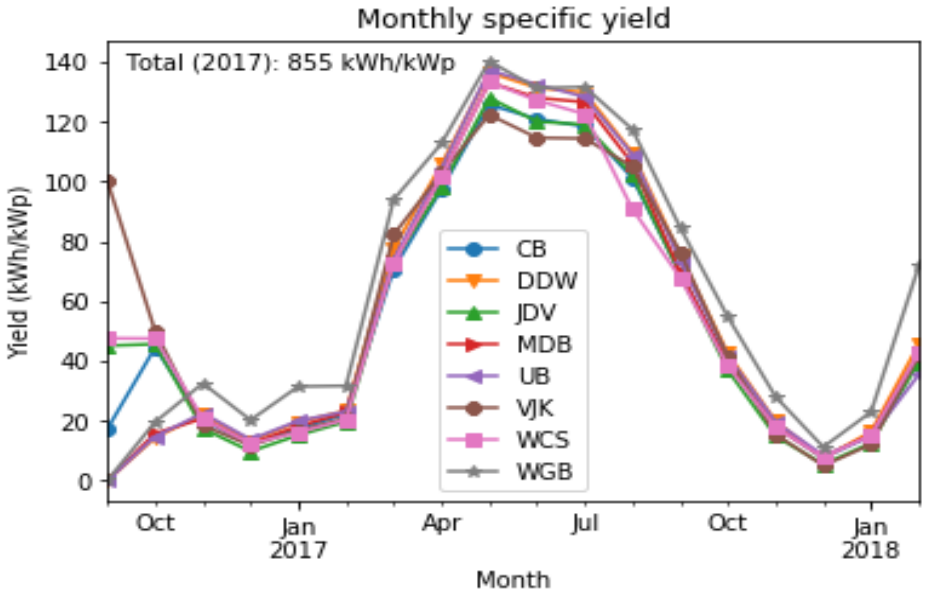

FIGURE 7 MONTHLY SPECIFIC YIELDS FOR EACH SYSTEM. FOR SOME SYSTEMS, ENERGY PRODUCTION MEASUREMENTS STARTED BETWEEN SEPTEMBER AND NOVEMBER 2016, HENCE THE SPREAD IN VALUES IN THIS PERIOD

As can be seen in the figure, most systems have comparable monthly specific yields. Throughout the year, the WGB system has the highest specific yield. This is the only system with a single southward orientation and a larger tilt angle of 30 degrees, which is closer to the optimal in The Netherlands (van Sark, Bosselaar et al. 2014). During summer differences in specific yields are larger. However, yearly values are within a range of 10% of each other, except for the WGB system. Yearly specific yields for each system are displayed in Table 2.

TABLE 2 YEARLY SPECIFIC YIELDS FOR EACH SYSTEM AND THE TOTAL SYSTEM

system	**specific yield 2017 (kWh/kWp)**
CB	808
DDW	878
JDV	801
MDB	844
UB	871
VJK	817
WCS	816
WGB	969
Total system	855

Again, it is clear that the WGB system performs best. The specific yield is significantly higher than that of the other systems and higher than the average value for the Netherlands of 875 kWh/kWp (van Sark, Bosselaar et al. 2014). This again can be attributed to the tilt and orientation of this system. Most system have a specific yield of about 10% lower than the nationwide average. However, the average of the region where USP is located is only 854 (van Sark, Bosselaar et al. 2014). Hence, the specific yield of the total system, 855 kWh/kWp, is similar to the region average. The discrepancy between the nationwide average and the system average can be due to the system orientation. While most of the systems in the Netherland are orientated due south (van Sark, Bosselaar et al. 2014), only two systems on USP share this orientation. The specific yields found in this research differ significantly from the results in (van Sark, de Waal et al. 2017). This is due to the data used in this research. Results in (van Sark, de Waal et al. 2017) are based on inverter data, which contains many gaps and is therefore less reliable than the production data used in this research.

4.2 Performance ratio

Here, the results of the analysis of the energy production data described in section 3.3 are displayed. The results were obtained using power production data from November 2016 up to and including February 2018. The irradiance data ranges from September 2016 up to and including January 8 2018. After this date, the UPOT system was moved for maintenance. However, this dataset was not complete for the whole time span mainly due to maintenance during the period. After filtering out the irradiance data that did not meet the required minimum time resolution of 15 minutes as described in section 3.3.2, the irradiance data was reduced to 269 useful days. Using this data, the performance ratio of each system was calculated. The results are displayed in Table 3.

TABLE 3 PERFORMANCE RATIOS OF ALL SYSTEMS AND THEIR RESPECTIVE UNCERTAINTIES

system	PR
CB	0.83 ± 0.07
DDW	0.88 ± 0.07
JDV	0.79 ± 0.07
MDB	0.86 ± 0.07
UB	0.89 ± 0.08
VJK	0.75 ± 0.06
WCS	0.84 ± 0.07
WGB	0.91 ± 0.08

On average, the total system has a performance ratio of 0.86 ± 0.07. This is a weighted average using the installed capacity as a weight factor for each system. The average PR is close to the benchmark of 0.85 for well-performing systems (Reich, Mueller et al. 2012). Again, the results differ from the results in (van Sark, de Waal et al. 2017) due to the different datasets used in this research.

The WGB system performs considerably better than other systems. This is probably due to the fact that the WGB is the only system with a higher tilt angle of 30 degrees and a single southward orientation, while other systems have multiple orientations and lower tilts. The orientation of the WGB system is close to the optimal module orientation in the Netherlands which is southward with 35-40 degrees tilt (van Sark, Bosselaar et al. 2014). Furthermore, the WGB system is located the furthest from UPOT of all systems. Therefore, it is possible that the irradiance at the site is differing more from the UPOT irradiance than the uncertainty indicates, resulting in a overestimation of the PR. Figure 8 displays the PRs of all systems in the period from June 2017 up to October 2017.

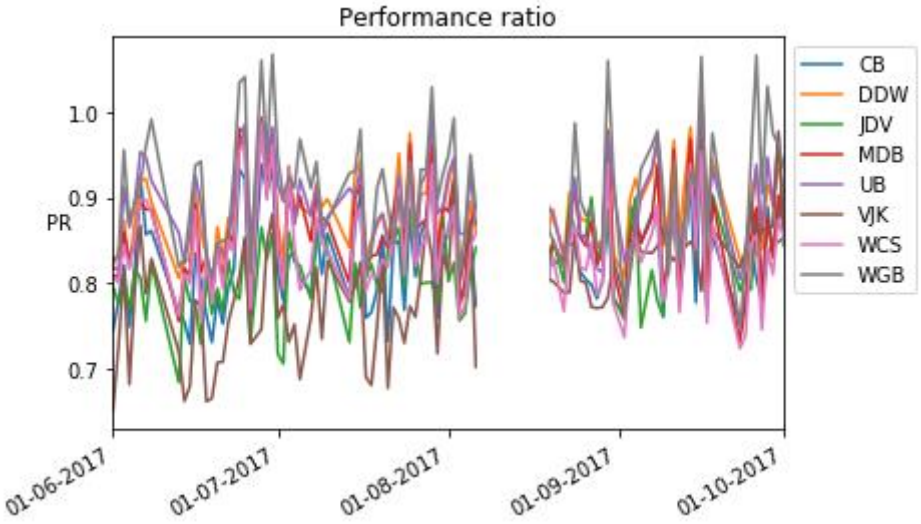

FIGURE 8 PERFORMANCE RATIO OF EACH SYSTEM. THE GAP IN AUGUST IS CAUSED BY MISSING IRRADIANCE DATA

As can be seen in Figure 8, there are some peaks in the PR of WGB that exceed 1.0. This is due to the high uncertainty in irradiance data. WGB is located the furthest away from the UPOT pyranometer, so the difference in irradiance on these day may be higher than the average of 4.9% between UPOT and the KNMI. Figure 9 displays the average monthly PR for each system. The figure starts at April since there is no irradiance data available for January – March.

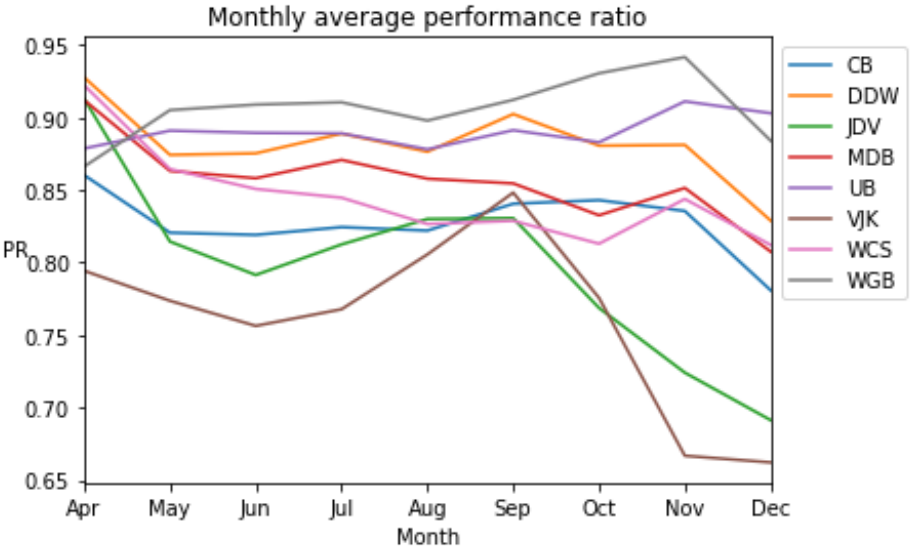

FIGURE 9 MONTHLY AVERAGE PERFORMANCE RATIO OF EACH SYSTEM IN THE MONTHS APRIL – DECEMBER

Again it is clear from Figure 9 that the WGB is the best performing system overall. Notable is the drop in PR in November (for two systems September) when irradiance drops. This can possibly be caused by unwanted shading by other buildings or obstacles at lower solar angles. The slightly lower efficiency of the modules at lower irradiance (Jinko Solar 2015) can amplify this drop in PR. This decrease in efficiency can be countered by an increase in efficiency due to lower cell temperatures in winter. However, there is no reliable cell temperature data available to support this. The missing irradiance data from winter may have a positive effect on the averaged PRs, assuming that the PR in January, February and March is comparable to the PR in November and December.

The VJK and JDV systems perform the worst. This can be caused by shading, soiling, high ambient and module temperatures and numerous other factors. One of the causes that should be visible in the inverter data is clipping by the inverters, which happens when the inverter load ratio (ILR) is high. The ILR is the ratio of the installed PV capacity and the inverter capacity. When analysing inverter data, clipping was found at the systems with the highest ILRs: the JDV system and the DDW system with ILRs of 1.366 and 1.336 respectively. When analysing available inverter data, 83 and 46 clipping instances where found for the JDV and DDW systems. This limits the yield of the system. For the VJK system, no clipping was found. This is due to the inverter capacity being almost equal to the PV capacity, with an ILR of 1.003. however, some inverter malfunctions were found in the error logs, which caused some loss in yield. Figure 10 displays the inverter time series of the JDV and DDW systems on a day where clipping occurred.

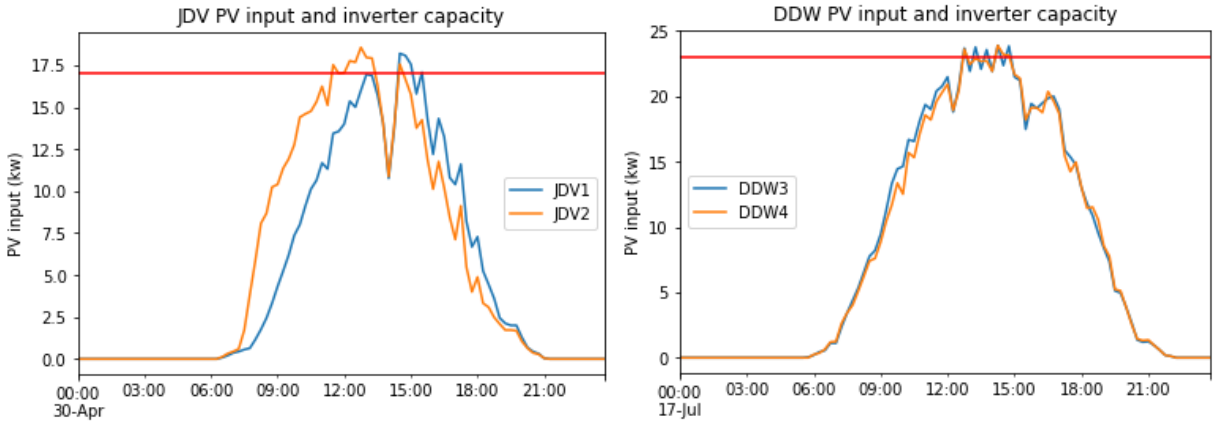

FIGURE 10 CLIPPING IN THE JDV AND DDW SYSTEMS. THE RED LINES INDICATE THE INVERTER CAPACITY OF THE INVERTERS THAT CAUSED CLIPPING

As can be seen in the figure, PV input to the inverter exceeds the inverter capacity (red line). In total, 11.7 and 6.2kWh was not utilised by the JDV and DDW systems during 2017 due to this effect. However, the totals are based on the inverter data, which has many gaps and missing days. Therefore it is probable that more clipping has taken place but has not been recorded properly. According to Good, Johnson (2016) generation losses at ILR around 1.35 are approximately 2%. Therefore, the specific yield and PR of the JDV and DDW systems could be approximately 2% higher. However, this would increase the investment costs, which may not be worth the small increase in yield.

It was proposed that the south-facing modules of the UB system perform better than the modules orientated northwards, and therefore the performance of the UB system could be increased by altering the orientation. This was verified by analysing individual inverter data of the UB system. However the differences between the individual inverters were not statically significant, even when ignoring uncertainty. Therefore the results from this analysis are omitted from this section.

The uncertainties of ~10% displayed in Table 3 are high. This is a results of the distance between the systems and the pyranometer, thus the high uncertainty in irradiance. This can be greatly reduced by placing pyranometers at every system.

4.3 Self-consumption

The results of the calculations of the self-consumption were obtained using power production and building electricity demand data from November 2016 up to and including February 2018. The average self-consumption is displayed in Table 4.

TABLE 4: AVERAGE SELF-CONSUMPTION OF EACH SYSTEM

system	self-consumption (%)
CB	100
VJK	100
WCS	100
DDW	100
UB	100
JDV	100
WGB	99 ± 1
MDB	100

As displayed in Table 4, the self-consumption of nearly all systems is 100%. The only exception is the WGB system, with a self-consumption of 99%. The high self-consumption of the buildings can be attributed to the high (base) demand of the buildings in to system capacity. In most cases, the electricity demand is much higher than peak production, so all energy is consumed in the building itself. The demand and PV production of DDW and UB are visualised in Figure 11.

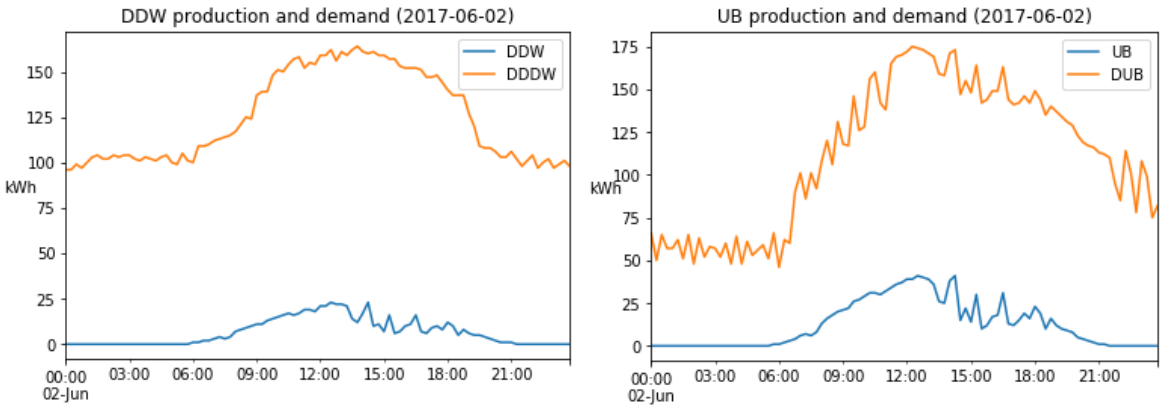

FIGURE 11 ELECTRICITY DEMAND CURVES (ORANGE) AND PV PRODUCTION CURVES (BLUE) OF THE DDW AND UB BUILDINGS. PEAKS CLEARLY COINCIDE IN THE UB FIGURE.

For all systems with self-consumption of 100%, the production and demand curves look similar to Figure 11, where the demand is always higher than (peak) production. However, this was not the case for the WGB system. The WGB is not a university or office building, but a stable that shelters cattle for the veterinary faculty. Therefore the demand profile of the WGB building is expected to be different. Furthermore, the building is small and has a large capacity PV system installed. It was expected that self-consumption of the WGB system would be lower during summer. Table 5 displays the monthly self-consumption of the WGB system. The self-consumption in summer is indeed lower, as expected. When further analysing the WGB data, something odd was found.

TABLE 5 MONTHLY SELF-CONSUMPTION OF THE WGB SYSTEM

month	self-consumption
1	99.8
2	99.4
3	98.8
4	98.75
5	98.2
6	98.35
7	98.2
8	98.1
9	98.6
10	99.15
11	99.3
12	99.8

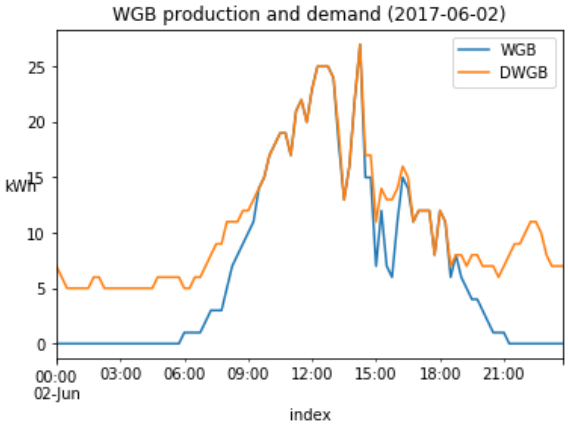

FIGURE 12 ELECTRICITY DEMAND (ORANGE) AND PV PRODUCTION OF WGB SYSTEM. PEAKS CLEARLY COINCIDE AND PV PRODUCTION NEVER EXCEEDS ELECTRICITY DEMAND

As displayed in Figure 10 the demand and PV production show great similarities. Demand and peak PV production coincide. This could be explained by the presence of a demand-side managing system that stores or consumes all produced PV energy. However, no such system is installed. After consulting with the UU energy coordinator, it was found that the demand data was erroneous. The demand data provided was the sum of the electricity demand from the grid (thus not the total electricity demand) and the produced PV energy. This explains the coinciding peaks in Figure 11 and Figure 10. The correct grid demand and production curves for the UB and WGB systems are displayed in Figure 13.

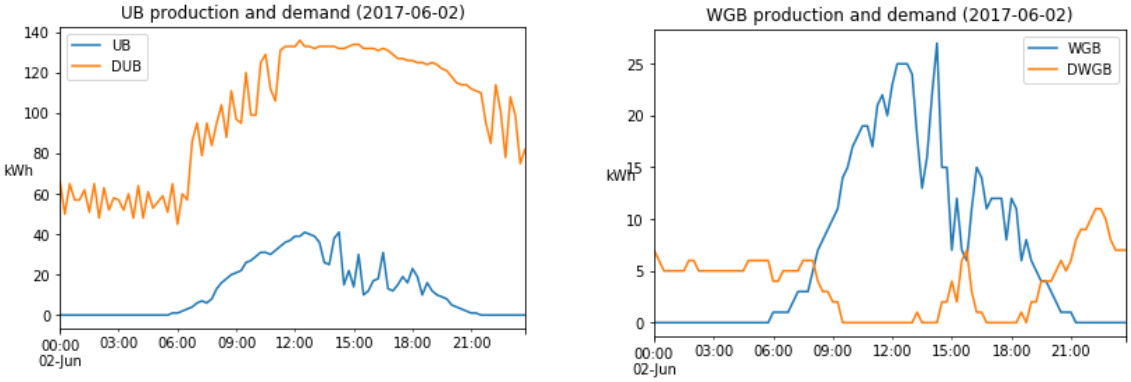

FIGURE 13 CORRECTED GRID DEMAND (ORANGE) AND PV PRODUCTION CURVES FOR THE UB AND WGB SYSTEM. PEAKS IN PRODUCTION NOW CAUSE DIPS IN GRID DEMAND, WHICH IS MOST CLEARLY VISIBLE IN THE FIGURE FOR THE WGB SYSTEM. HERE, HIGH PV PRODUCTION REDUCES GRID DEMAND TO 0.

The demand data being the grid demand does not have much impact on the results in Table 4. All systems with 100% self-consumption such as the UB and DDW systems displayed in Figure 11 have no points where the grid demand is zero (or the demand equals the production in the old data) , meaning that all the produced PV energy is consumed. This does not depend on which data was used. However, this does not hold for the WGB system. Points with zero grid demand indicate that the electricity demand is being satisfied by the PV production. This does not mean that *all* PV energy is being consumed by the building itself. There may be a surplus that is delivered to the grid. Unfortunately, there is no meter installed yet to measure this surplus. Therefore, it is impossible to give a value for the self-consumption of the WGB system. However in summer, when the PV production is higher, there are more points with zero grid demand. Hence it is still likely that self-consumption is lower in summer. For quantitative results on the self-consumption of the WGB system, a meter that measures electricity delivered back to the grid should be installed.

Since the self-consumption is high, it is interesting to get insight into what part of the demand is satisfied by the PV production. This was calculated for each system, including WGB, where 100% self-consumption was assumed to make this calculation possible. The daily PV/demand ratio is displayed in Figure 14.

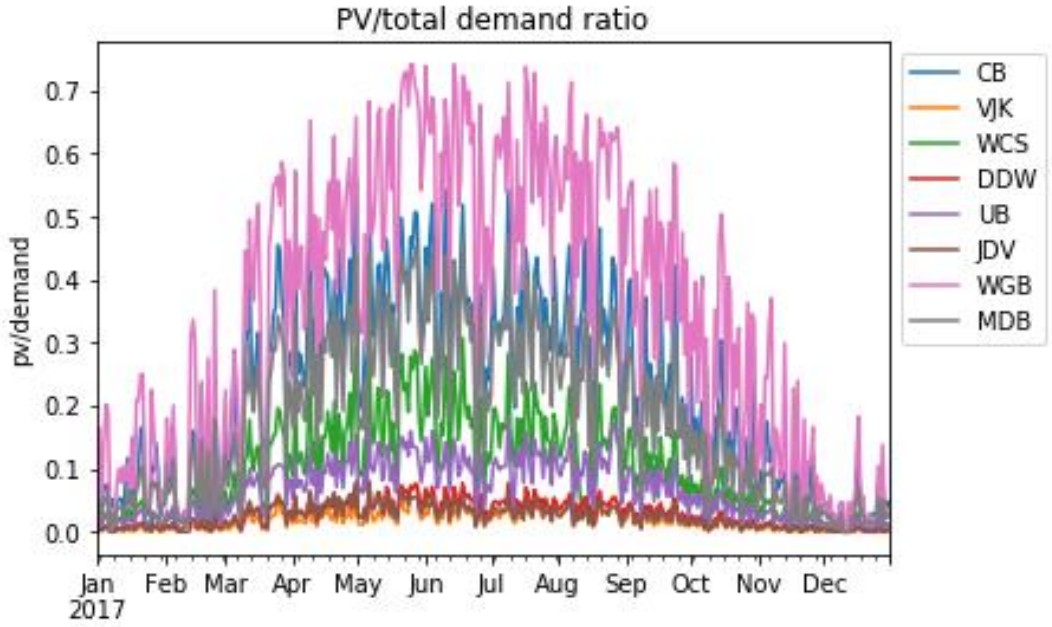

FIGURE 14 PV/TOTAL DEMAND RATIO FOR EACH SYSTEM OVER THE YEAR 2017. THE SHAPE SHOWS SIMILARITIES TO DAILY IRRADIANCE CURVES.

It is clear that the WGB building has the highest PV/demand ratio throughout the year. This is due to the relatively high performance of this system and the low electricity demand of the building. However, 100% self-consumption was assumed, which is most probably an overestimation. Therefore it is likely that the PV/demand ratio of the WGB is lower in reality. However, since there is no data available for electricity delivered back to the grid (or negative demand) there is no manner to obtain more accurate results. The PV/demand ratio is higher. The daily total demand for each building is displayed in Figure 15.

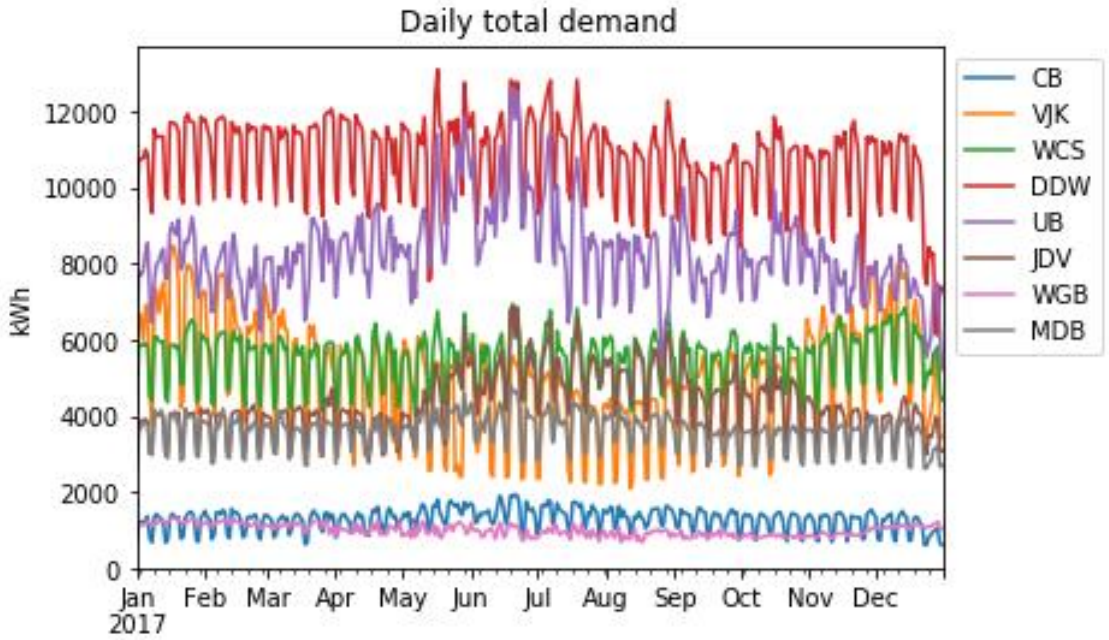

FIGURE 15 DAILY TOTAL ELECTRICITY DEMAND OF THE BUILDINGS THAT HAVE A PV SYSTEM INSTALLED. PERIODICAL DIPS ARE CAUSED BY LOWER DEMAND IN THE WEEKEND.

The daily total demand is fairly constant over the year. Some buildings show a peak in demand during summer, which is likely due to increased cooling demand due to high ambient temperatures. However, this has a decreasing effect on the PV/demand ratio. Therefore, the high PV/demand ratio during summer can be attributed solely to the high PV production. Table 6 displays average values for the PV/demand ratio for each building and for the total system, over 2017.

TABLE 6 AVERAGE PV/DEMAND RATIOS FOR EACH SYSTEM AND THE TOTAL SYSTEM

Building	PV/demand
CB	0.22
VJK	0.02
WCS	0.10
DDW	0.03
UB	0.06
JDV	0.02
WGB	0.35
MDB	0.18
Total system	0.16

The PV production satisfies 16% of the total demand of the buildings. This is much higher than the 2% stated in section 1.1. However the 2% is based on the total energy demand of the UU as a whole, while the 16% is only of the buildings that have a PV system installed. The vast majority of the UU buildings have no PV system.

4.4 Correlation

The results obtained using the methods described in section 3.5 are discussed in this section. First the decorrelation lengths for both the 5 and 15-minute data sets are discussed.

4.4.1 Decorrelation length

Both 5 and 15-minute inverter data was used to calculate the decorrelation length of the system. Due to the fact that 5-minute data gets replaced by 15-minute data after one month, the timespan of the 5-minute data is limited to December 22 2017 up to and including march 22 2018. For the 15-minute data, only days without any of the aforementioned gaps were used. The complete 15-minute data from the production meters was sued as well.

4.4.1.1 5-minute data

Using the 5-minute data, the weighted average decorrelation length is 2.19±0.31 km, which is in the range of the results of (Elsinga, Van Sark 2013). Within the daily results, values for clear days were higher. This is caused by the low perpendicular variance in the data, resulting in a flat curve. Figure 16 displays data from a clear day and the corresponding fit to the exponential curve.

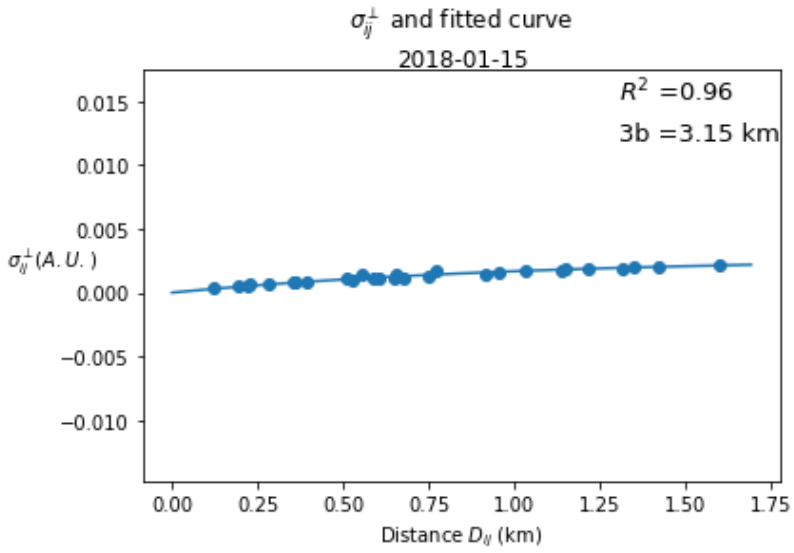

FIGURE 16 PERPENDICULAR STANDARD DEVIATION OF SYSTEM PAIRS PLOTTED AGAINST THE INTER-SYSTEM DISTANCE AND THE FITTED EXPONENTIAL CURVE ON A CLEAR DAY, USING 5-MINUTE DATA

The high value of R^2 combined with the high value of the decorrelation length results in a higher average decorrelation length, since the R^2 values are used as weights in calculating the average.

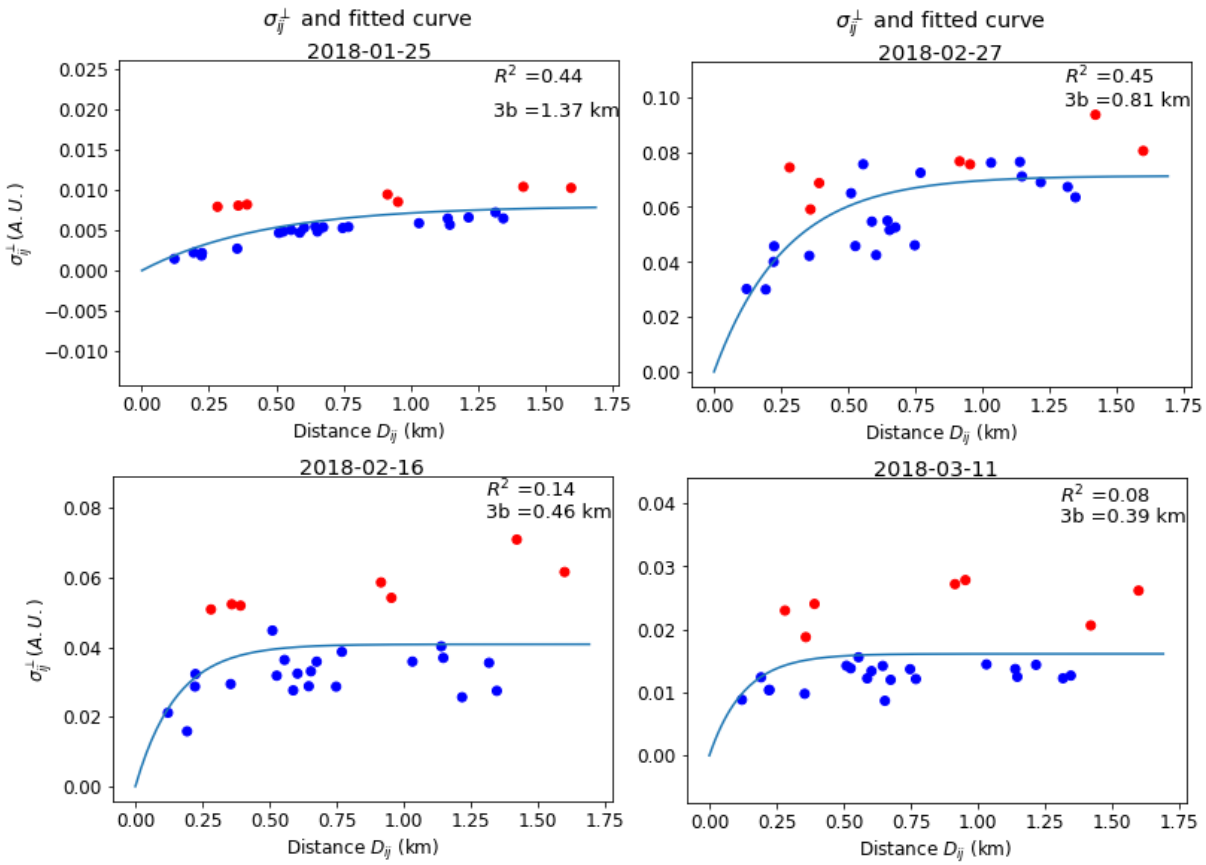

FIGURE 17 PERPENDICULAR STANDARD DEVIATION OF SYSTEM PAIRS PLOTTED AGAINST THE INTER-SYSTEM DISTANCE AND THE FITTED EXPONENTIAL CURVE ON CLOUDY DAYS, USING 5-MINUTE DATA. RED POINTS INDICATE SYSTEM PAIRS WITH THE WGB SYSTEM.

Figures of cloudy days similar to Figure 17 show a notable similarity. The points highlighted in red are high above the curve for each day, increasing the resulting value for the decorrelation length. When studying these points more closely, it turned out that it were the points corresponding to pairs with the WGB system. This is the only system with 30 degree tilt combined with a southward orientation. This makes the system more sensitive to direct radiation, and therefore more sensitive to fluctuations in irradiance due to cloud movement. Omitting the WGB system from the data would reduce the decorrelation length, however it would not be justifiable to do so just to reduce the decorrelation length. Therefore, the weighted average decorrelation length for this system is 2.19±0.31 km. When taking the average without weights, the decorrelation length was found to be 1.62±0.28 km. The largest inter-system distance D_{ij} is 1.60 km. Hence, regardless of which averaging method was used, all pairs have an inter-system distance smaller than the decorrelation length. Therefore the Pearson correlation coefficient was calculated for each pair. This is discussed in section 3.5.2. The limited time span of the 5-minute data explains the lack of seasonal analysis of the decorrelation length.

4.4.1.2 15-minute data

The 15-minute inverter data that replaced old 5-minute data was used to calculate the decorrelation length with a 15-minute time step. In total, this dataset consists of 181 days without missing data points. Using this data resulted in a weighted average decorrelation length of 609±699454 km. This result suggests there is no correlation at all, but it is unreliable. First of all, the uncertainty is extremely large compared to the result. The uncertainty originates from fitting the curve. These fits done on the perpendicular standard deviation were of very low quality, causing this large uncertainty. Daily values of the decorrelation length varied between 16000 and 0.02 km. The best fit had an R^2 of 0.5, while some values for R^2 were negative, meaning that a straight line would result in a better fit. Figure 18 displays data from a day with a negative R^2.

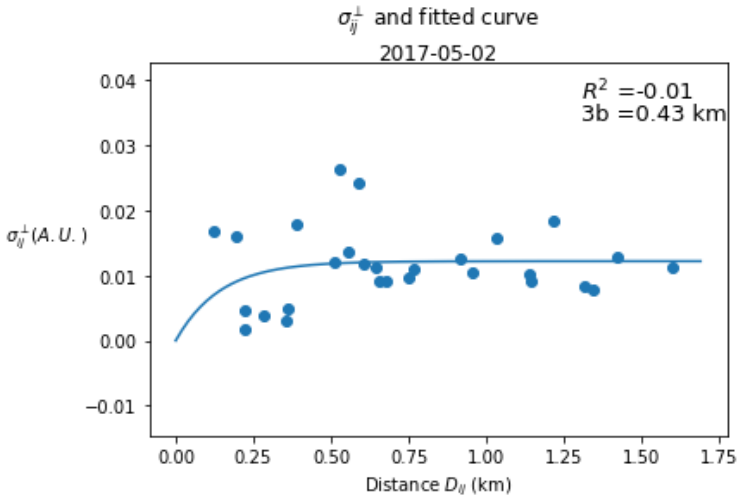

FIGURE 18 PERPENDICULAR STANDARD DEVIATION OF SYSTEM PAIRS PLOTTED AGAINST THE INTER-SYSTEM DISTANCE AND THE FITTED EXPONENTIAL CURVE ON A CLOUDY DAY USING 15-MINUTE DATA

The resulting low decorrelation length in Figure 18 of 0.43 km is caused by the data having no clear correlation between $\sigma_{ij}^{\perp}$ and D_{ij}. A straight line would result in a better fit, and therefore 3b is small so that the exponential curve reaches the plateau, which is approximately a straight line, at low D_{ij}. The low quality results can be explained by the lack of data with $D_{ij} > 1.60$ km. Lower time resolution makes the $\sigma_{ij}^{\perp}$ more smooth over distance. This is because events causing points where $\sigma_i \neq \sigma_j$, usually clouds, can cover more distance during a larger timestep hence smoothing the data. Figure 19 displays a zoomed out fitted curve with a large decorrelation length.

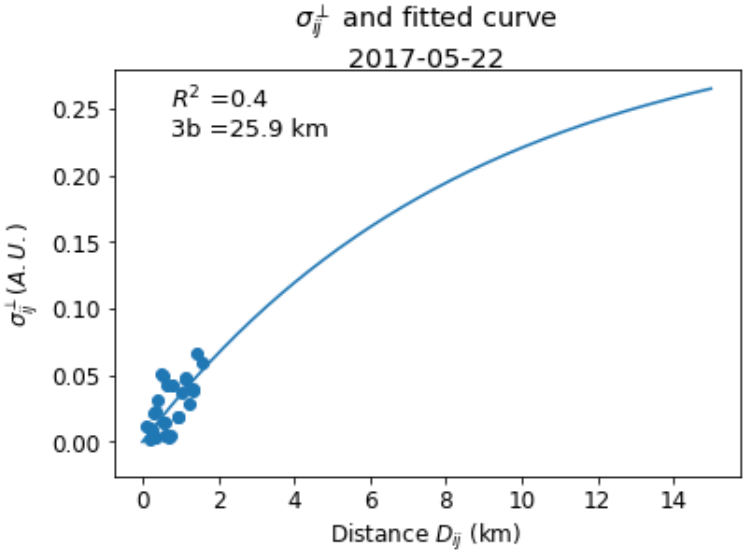

FIGURE 19 PERPENDICULAR STANDARD DEVIATION AND THE FITTED EXPONENTIAL CURVE USING 15-MINUTE DATA. THE LACK OF DATA AT D>1.6 AND ITS IMPLICATIONS ARE CLEAR FROM THIS FIGURE

With the largest inter-system distance being 1.6 km, no data for larger distances is available. However, this is needed to make reliable fits. As can be seen in the figure, the start of the curve seems to fit the data. However, data with $D_{ij} > 1.60$ km is needed to calculate a reliable decorrelation length for 15-minute time resolution data. This data was not available and not relevant for the USP system since the largest inter-system distance is only 1.60 km. There is no way of knowing if the fitted curve is correct at $D_{ij} > 1.6$ km. Therefore the results of this analysis are inconclusive. However, based on (Elsinga, Van Sark 2013) one thing can be stated with relative certainty. For larger timestep data, the decorrelation length will be larger. Therefore, the Pearson correlation coefficient was calculated using the 15-minute data. This is discussed in the next section.

4.4.2 Pearson correlation

The average Pearson correlation coefficient for each system pair were calculated using the available 5 and 15-minute data. Results are displayed below.

TABLE 7 AVERAGE PEARSON CORRELATION COEFFICIENTS FOR EACH SYSTEM PAIR POWER SERIES CALCULATED USING THE 5-MINUTE DATA FROM DECEMBER 22 2017 UP TO MARCH 22 2018

	CB	DDW	JDV	MDB	UB	VJK	WCS	WGB
CB	1	0.973	0.965	0.97	0.973	0.975	0.972	0.943
DDW	0.973	1	0.977	0.976	0.983	0.964	0.981	0.953
JDV	0.965	0.977	1	0.989	0.972	0.963	0.989	0.955
MDB	0.97	0.976	0.989	1	0.977	0.957	0.991	0.966
UB	0.973	0.983	0.972	0.977	1	0.956	0.978	0.951
VJK	0.975	0.964	0.963	0.957	0.956	1	0.958	0.928
WCS	0.972	0.981	0.989	0.991	0.978	0.958	1	0.966
WGB	0.943	0.953	0.955	0.966	0.951	0.928	0.966	1

It is clear from Table 7 that each system pair has high correlation. Systems like the WCS and MDB systems, which are close to each other and have similar layouts ,approach the autocorrelation of 1. Overall, the WGB system has the lowest correlation with the other systems, which can be explained by the different system layout with a tilt of 30 degrees and a single southward module orientation. Furthermore, the WGB system is the furthest from other systems and UPOT. The VJK system has the second lowest correlation. This system also has a single southward orientation, causing higher sensitivity to direct irradiance and therefore lower correlation.

TABLE 8 AVERAGE PEARSON CORRELATION COEFFICIENT FOR EACH SYSTEM PAIR POWER SERIES USING THE AVAILABLE 15-MINUTE DATA

	CB	DDW	JDV	MDB	UB	VJK	WCS	WGB
CB	1	0.999	0.997	0.998	0.999	0.995	0.997	0.988
DDW	0.999	1	0.999	0.999	1	0.995	0.999	0.989
JDV	0.997	0.999	1	0.999	0.998	0.995	0.998	0.988
MDB	0.998	0.999	0.999	1	1	0.992	0.999	0.986
UB	0.999	1	0.998	1	1	0.992	0.999	0.987
VJK	0.995	0.995	0.995	0.992	0.992	1	0.991	0.993
WCS	0.997	0.999	0.998	0.999	0.999	0.991	1	0.984
WGB	0.988	0.989	0.988	0.986	0.987	0.993	0.984	1

The correlation coefficients displayed in Table 8 are even higher than those in Table 7. This is due to the smoothing of the data due to the larger time step. Peaks and dips in the 5-minute data are now averaged in the 15-minute data, creating smoother data and increasing correlation. The same behaviour of the WGB and VJK systems is also present in Table 7. Table 7 and 7 clearly show very high correlation between each system pair. The coefficients are comparable to the coefficients found for a large single system of several megawatts, which averaged at 0.97 for 5-minute data (Shedd, Hodge et al. 2012). Moreover, the system pair correlation is very close to the correlation of the inverters in the MDB system, displayed in Table 9 and 10, which is the largest system on Utrecht Science Park.

TABLE 9 AVERAGE PEARSON CORRELATION COEFFICIENTS OF THE INVERTERS OF THE MDB SYSTEM, CALCULATED USING 5-MINUTE DATA. VALUES ARE VERY CLOSE TO THAT DISPLAYED IN TABLE 4

	MDB1	MDB2	MDB3	MDB4	MDB5	MDB6	MDB7	MDB8
MDB1	1	0.971	0.986	0.973	0.975	0.973	0.973	0.968
MDB2	0.971	1	0.989	0.999	0.972	0.995	0.962	0.988
MDB3	0.986	0.989	1	0.991	0.987	0.989	0.982	0.986
MDB4	0.973	0.999	0.991	1	0.974	0.996	0.964	0.99
MDB5	0.975	0.972	0.987	0.974	1	0.971	0.996	0.982
MDB6	0.973	0.995	0.989	0.996	0.971	1	0.962	0.991
MDB7	0.973	0.962	0.982	0.964	0.996	0.962	1	0.975
MDB8	0.968	0.988	0.986	0.99	0.982	0.991	0.975	1

TABLE 10 AVERAGE PEARSON CORRELATION COEFFICIENTS OF THE INVERTERS OF THE MDB SYSTEM, CALCULATED USING 15-MINUTE DATA. VALUES ARE VERY CLOSE TO THAT DISPLAYED IN TABLE 5

	MDB1	MDB2	MDB3	MDB4	MDB5	MDB6	MDB7	MDB8
MDB1	1	0.997	1	0.997	0.999	0.995	0.999	0.996
MDB2	0.997	1	0.998	1	0.995	0.999	0.997	0.999
MDB3	1	0.998	1	0.998	0.999	0.997	0.999	0.997
MDB4	0.997	1	0.998	1	0.995	0.999	0.997	0.999
MDB5	0.999	0.995	0.999	0.995	1	0.993	0.999	0.995
MDB6	0.995	0.999	0.997	0.999	0.993	1	0.995	0.998
MDB7	0.999	0.997	0.999	0.997	0.999	0.995	1	0.997
MDB8	0.996	0.999	0.997	0.999	0.995	0.998	0.997	1

The degree of correlation between the systems is important when modelling and forecasting the yield of the system. Marcos et al. (2016) propose a method of modelling several systems as one system, with a irradiance meter located at one system. However, this method relies on power fluctuations being smoothed by larger inter-system distances and thus low correlation. This does not apply to the USP system. When comparing tables 7 and 8 to tables 9 and 10, it can be concluded that the total USP system has comparable correlation to that of a single system. Therefore, when modelling and forecasting the USP system can be treated as one single system, especially when using a 15-minute time resolution.

5 Conclusion & discussion

Based on the yearly specific yield it can be concluded that the USP PV system performs as expected. While the average value (855 kWh/kWp) is slightly below the average of The Netherlands (875), it is very close to the average value of the Utrecht area (854)(van Sark 2014). It was expected that the system would produce approximately 1 million kWh. The annual yield in 2017 was 1.04 million kWh, which meets expectations. When looking at the performance ratio of the system, the same can be concluded. The average PR is 0.86 ± 0.07, which is close to the benchmark of 0.85 for well performing systems (Reich, Mueller et al. 2012). Results differ significantly from the results displayed in (van Sark, de Waal et al. 2017). The production data used in this research contains no gaps as opposed to the data used in (van Sark, de Waal et al. 2017). Therefore the results of this research are more reliable. The PR and specific yield of some systems is below expectations. For the JDV and DDW system, part of this can be explained by clipping due to limited inverter capacity. The inverter of the VJK system has had some malfunctions in the analysed time period, reducing its PR and yield. When comparing PRs with similar research (Kausika, Moraitis et al. 2018; Moraitis, Kausika et al. 2018; IEA-PVPS 2014), the PRs of the individual systems are within the margin of error of the averages found for systems in the Netherlands and Europe. The WGB system clearly performs best. It has the highest specific yield and the highest PR. This can be attributed to the system tilt and orientation. One could argue that system performance would increase if all systems would have the same orientation and tilt as the WGB system. While this is probably true, it is not the goal of the UU to increase performance. The goal is to produce sustainable energy (UU, 2017), thus have high PV yield. All systems except the WGB system are located on flat roofs. Increasing the module tilt and changing the orientation would require more spacing between arrays due to shading, thus reducing the installed capacity and decreasing yield. The uncertainty of the PR analysis is high. This is largely due to the uncertainty in irradiance caused by the distance between the systems and UPOT. To present more accurate results, a pyranometer should be installed at each system. This would significantly decrease uncertainty in irradiance data. These pyranometers will be installed in the coming months. Thus the PRs should be calculated again after enough data has been gathered in approximately a year. It is expected that the average values will be lower than those found in this research. The PR is lower in months with lower irradiance, while irradiance data of January to April is missing. The expected lower PRs during these months would decrease the yearly average.

The self-consumption of all but one if the systems is 100%, which was expected by (IEA-PVPS 2016). The electricity demand of these buildings is higher than peak PV production, thus the electricity demand from the grid never drops to 0. The only exception is the WGB system, where the grid demand regularly drops to 0. Energy delivered back to grid is not measured at this location therefore a quantitative analysis of the self-consumption of this building cannot be done. However it is expected that the self-consumption of the WGB system is below 100%. Based on the available data, PV/demand ratio of the total system is 16%. However, due to the lack of data on the excess PV production by the WGB system, this is probably slightly lower in reality.

All inter-system distances are lower than the decorrelation length of 2.19 ± 0.31 km, which was found using the 5-minute data. This result is in agreement of similar research (Elsinga, Van Sark 2013). The systems correlate strongly with each other. The WGB system has an increasing effect on the decorrelation length, caused by the stronger responses to fluctuations in irradiance due to the system orientation and tilt. The dataset used to calculate the decorrelation length was limited. Therefore, seasonal effect on the decorrelation length could not be analysed. When more 5-minute data is available, the decorrelation length, including seasonal variations, should be analysed again.

The 15-minute data proved to be unsuitable to calculate the decorrelation length. The lack of data with an inter-system distance greater than 1.6 km caused the exponential curve fits to be of very poor quality. Thus, no feasible results were obtained in this analysis. Based on similar research, it can be stated that the decorrelation length using 15-minute data will be larger than the result found using 5-minute data, due to smoothing effects of the longer time step. Hence, all inter-system distances are smaller than the decorrelation length and strong correlation is expected. This strong correlation was indeed found when calculating the Pearson correlation of the power production time series. The values found using 5-minute data are comparable to that of individual

inverters in a large system, and even to that of the largest system on USP. When using the 15-minute data, the correlation was even larger. Correlation coefficients found are close to one, and even closer to that of the individual inverters in the MDB system. Therefore it can be concluded that the USP PV system can be modelled as one system in forecasting especially when using a 15-miute timestep.

All in all it can be concluded that the USP PV system performs well. Correlation between the systems are very high, and therefore the total system can be treated as one system, especially when using a 15-minute time step. For more robust conclusion, higher quality irradiance data and power production data (specifically 5-minute data) should be gathered, and the analyses done in this research should be repeated using this data. To facilitate the repetition of these analyses when more data is available, a cleaned up version of the code used in this research will be made available.

6 Acknowledgements

I would like to thank Wilfried van Sark, my supervisor, for giving me the opportunity to conduct this research and to do so at my own pace. Thanks go out to Atse Louwen for providing the irradiance data from UPOT, pointing me towards the pvlib software and helping me with some small issues. Thanks to Mariska Ruiter of Profinrg for giving me access to the NetEco portal swiftly after asking for this. Thanks to Hans de Valk, also of Profinrg, for providing some technical details of the USP systems. Thanks to the UU energy coordinator, Oswin Carboex, for providing the production meter data and for confirming that the data contained errors quickly after this was found. I would also like to thank everyone at Stackoverflow for helping met with coding problems.

7 References

CBS STATLINE, 2018, hernieuwbare elektriciteit; productie en vermogen [06/01, 2018].

ELSINGA, B. and SARK, W., 2015. Spatial power fluctuation correlations in urban rooftop photovoltaic systems. *Progress in Photovoltaics: Research and Applications,* **23**(10), pp. 1390-1397.

ELSINGA, B. and VAN SARK, W.G., 2017. Short-term peer-to-peer solar forecasting in a network of photovoltaic systems. *Applied Energy,* .

ELSINGA, B. and VAN SARK, W.G., 2013. Power Output Variability in randomly spaced dutch urban rooftop solar photovoltaic systems, *Photovoltaic Specialists Conference (PVSC), 2013 IEEE 39th* 2013, IEEE, pp. 1794-1798.

GOOD, J. and JOHNSON, J.X., 2016. Impact of inverter loading ratio on solar photovoltaic system performance. *Applied Energy,* **177**, pp. 475-486.

HOFF, T.E. and PEREZ, R., 2010. Quantifying PV power output variability. *Solar Energy,* **84**(10), pp. 1782-1793.

HOLMGREN, W.F., ANDREWS, R.W., LORENZO, A.T. and STEIN, J.S., PVLIB python 2015.

IEA-PVPS, 2018. snapshot of global photovoltaic markets.

IEA-PVPS, 2016. review and analysis of PV self-consumption policies.

IEA-PVPS, 2014. analytical monitoring of grid-connected photovoltaic systems.

JINKO SOLAR, 2015. *JKM270PP-60 255-270 Watt poly crystalline module specifications.*

KAUSIKA, B.B., MORAITIS, P. and VAN SARK, W.G., 2018. Visualization of Operational Performance of Grid-Connected PV Systems in Selected European Countries. *Energies,* **11**(6), pp. 1330.

MARCOS, J., PARRA, Í, GARCÍA, M. and MARROYO, L., 2016. Simulating the variability of dispersed large PV plants. *Progress in Photovoltaics: Research and Applications,* **24**(5), pp. 680-691.

MORAITIS, P., KAUSIKA, B.B., NORTIER, N. and VAN SARK, W., 2018. Urban Environment and Solar PV Performance: The Case of the Netherlands. *Energies,* **11**(6), pp. 1333.

PEREZ, R., KIVALOV, S., SCHLEMMER, J., HEMKER, K. and HOFF, T., 2011. Short-term irradiance variability: Station pair correlation as a function of distance. *Solar Energy,* **85**(7), pp. 1343-1353.

PEREZ, R., KIVALOV, S., SCHLEMMER, J., HEMKER, K. and HOFF, T.E., 2012. Short-term irradiance variability: Preliminary estimation of station pair correlation as a function of distance. *Solar Energy,* **86**(8), pp. 2170-2176.

PERPIÑÁN, O., MARCOS, J. and LORENZO, E., 2013. Electrical power fluctuations in a network of DC/AC inverters in a large PV plant: Relationship between correlation, distance and time scale. *Solar Energy,* **88**, pp. 227-241.

REICH, N.H., MUELLER, B., ARMBRUSTER, A., SARK, W.G., KIEFER, K. and REISE, C., 2012. Performance ratio revisited: is PR> 90% realistic? *Progress in Photovoltaics: Research and Applications,* **20**(6), pp. 717-726.

REINDERS, A., VERLINDEN, P., VAN SARK, W. and FREUNDLICH, A., 2017. *Photovoltaic Solar Energy: From Fundamentals to Applications.* John Wiley & Sons.

RVO, 2017. SDE+ spring 2017.

SHEDD, S., HODGE, B., FLORITA, A. and ORWIG, K., 2012. *Statistical Characterization of Solar Photovoltaic Power Variability at Small Timescales: Preprint,* .

UU,2017 , Duurzame UU. Available: https://www.uu.nl/organisatie/duurzame-uu [October 20, 2017].

VAN SARK, W., 2014. opbrengst van zonnestroomsystemen in Nederland.

VAN SARK, W., DE WAAL, A., UITHOL, J., DOLS, N., HOUBEN, F., KUEPERS, R., STERRENBURG, M., VAN LITH, B. and BENJAMIN, F., 2017. Energy performance of a 1.2 MWp photovoltaic system distributed over nine buildings at Utrecht University campus, *Proceedings of the 33rd European Photovoltaic Solar Energy Conference* 2017, WIP-Renewable Energies, pp. 2284-2287.

VAN SARK, W., BOSSELAAR, L., GERRISSEN, P., ESMEIJER, K., MORAITIS, P., VAN DEN DONKER, M. and EMSBROEK, G., 2014. Update of the Dutch PV specific yield for determination of PV contribution to renewable energy production: 25% more energy! *Proceedings of the 29th EUR-PSEC,* , pp. 4095-4097.

VAN SARK, W., DE WAAL, A., UITHOL, J., DOLS, N., HOUBEN, F., KEUPERS, R., SCHERRENBURG, M., VAN LITH, B. and BENJAMIN, F., 2017. Energy Performance of a 1.2MWp Photovoltaic System Distributed over Eight Buildings at Utrecht University Campus, 2017.